Photoinduced Processes in a Tricomponent Molecule Consisting of Diphenylaminofluorene−Dicyanoethylene−Methano[60]fullerene

Mohamed E. El-Khouly,[†,‡] Prashant Padmawar,[§] Yasuyuki Araki,[†] Sarika Verma,[§] Long Y. Chiang,*[,§] and Osamu Ito*[,†]

Institute of Multidisciplinary Research for Advanced Materials, Tohoku University, Katahira, Aoba-ku, Sendai980-8577, Japan, Department of Chemistry, Faculty of Education, Tanta University, Kafr El-Sheikh, Egypt, Department of Chemistry, Institute of Nanoscience and Engineering Technology, University of Massachusetts Lowell, 1 University Avenue, Lowell, Massachusetts 01854-5047

Received: September 19, 2005; In Final Form: November 18, 2005

Photoinduced intramolecular processes in a tricomponent molecule $C_{60}(>(CN)_2-DPAF)$, consisting of an electron-accepting methano[60]fullerene moiety ($C_{60}>$) covalently bound to an electron-donating diphenylaminofluorene (DPAF) unit via a bridging dicyanoethylenyl group [$(CN)_2$], were investigated in comparison with $(CN)_2-DPAF$. On the basis of the molecular orbital calculations, the lowest charge-separated state of $C_{60}(>(CN)_2-DPAF)$ is suggested to be $C_{60}^{\bullet-}(>(CN)_2-DPAF^{\bullet+})$ with the negative charge localized on the fullerene cage, while the upper state is $C_{60}(>(CN)_2^{\bullet-}-DPAF^{\bullet+})$. The excited-state events of $C_{60}(>(CN)_2-DPAF)$ were monitored by both time-resolved emission and nanosecond transient absorption techniques. In both nonpolar and polar solvents, the excited charge-transfer state decayed mainly through initial energy-transfer process to the C_{60} moiety yielding the corresponding $^1C_{60}$*, from which charge separation took place leading to the formation of $C_{60}^{\bullet-}(>(CN)_2-DPAF^{\bullet+})$ in a fast rate and high efficiency. In addition, multistep charge separation from $C_{60}(>(CN)_2^{\bullet-}-DPAF^{\bullet+})$ to $C_{60}^{\bullet-}(>(CN)_2-DPAF^{\bullet+})$ may be possible with the excitation of charge-transfer band. The lifetimes of $C_{60}^{\bullet-}(>(CN)_2-DPAF^{\bullet+})$ are longer than the previously reported methano[60]fullerene-diphenylaminofluorene $C_{60}(>(C=O)-DPAF)$ with the C_{60} and DPAF moieties linked by a methanoketo group. These findings suggest an important role of dicyanoethylenyl group as an electron mediating bridge in $C_{60}(>(CN)_2-DPAF)$.

Introduction

Studies on donor−acceptor systems capable of undergoing electron- or energy-transfer are of current interest to mimic the primary events of photosynthetic reaction center and to develop molecular electronic devices.[1,2] Toward constructing such systems, fullerenes are particularly appealing as electron acceptors, because of their three-dimensional structures, delocalized π-electron systems within the spherical carbon framework, small reorganization energy, low reduction potentials, and absorption spectra extending over most of the visible region.[3−5] The covalent linkage of fullerene (such as C_{60}) to a number of interesting electro- and photoactive species offers new opportunities in the design of new materials that produce long-lived charge-separated states in high quantum yields. Among various electron donors, fluorene-based materials are of particular interest, because of their thermal and chemical stability along with desirable photoluminescence and electroluminescence properties.[6] The unique chemical and physical characteristics of fluorene compounds[6] make them essential and accessible in a wide variety of applications ranging from the electroluminescent devices, plastic solar cells, and photodynamic therapy.[7,8]

A tremendous amount of attention has been made to the studies of photoinduced intramolecular electron-transfer processes of various C_{60} compounds covalently linked with electron-rich amines.[9−14] In our recent papers, two-photon excitation, photoinduced charge-separation (CS), and charge-recombination (CR) processes of $C_{60}(>(C=O)-DPAF)$, consisting of a C_{60} cage bonded with diphenylaminofluorene (DPAF) via a methanoketo group, were reported.[15,16] In this molecular system, the intramolecular charge-separation process was observed to occur via singlet excited state of the C_{60} moiety in polar solvents that generated the corresponding radical ion pairs $C_{60}^{\bullet-}(>(C=O)-DPAF^{\bullet+})$.[16] The lifetime ($\tau_{RIP}$) of $C_{60}^{\bullet-}(>(C=O)-DPAF^{\bullet+})$ was evaluated to be long (150 ns) in DMF despite a quite short value (<10 ns) in benzonitrile (PhCN). This order was interpreted by the Marcus theory.[17]

In this report, we describe synthesis and photophysics of 7-(1,2-dihydro-1,2-methano[60]fullerene-61-{1,1-dicyanoethylenyl})-9,9-di(methoxyethyl)-2-diphenylaminofluorene $C_{60}(>(CN)_2-DPAF)$, in which the DPAF and C_{60} moieties are interconnected with a dicyanoethylenyl group [$(CN)_2$]. On the C-9 position of fluorene, two methoxyethyl groups were introduced to increase the solubility of the material (Figure 1). For the purpose of comparison, 7-[1-(1,1-dicyanoethylene)-1-methyl]-9,9-dimethoxyethyl-2-diphenylaminofluorene [$(CN)_2-DPAF$] was also synthesized as a reference model compound. Photochemical events of all materials were investigated through the correlation among steady-state spectra, time-resolved fluorescence spectra, and nanosecond laser flash photolysis data taken in PhCN, *o*-dichlorobenzene (DCB), anisole (ANS), and toluene (TN).

Experimental Section

Materials. *Synthesis of 7-[1-(1,1-dicyanoethylene)-1-methyl]-9,9-dimethoxyethyl-2-diphenylaminofluorene (CN)$_2$−DPAF.* In a reaction flask, 7-acetyl-9,9-dimethoxyethyl-2-diphenylaminofluorene (500 mg, 1.0 mmol) and malononitrile (150 mg, 2.2

[†] Tohoku University.
[‡] Tanta University.
[§] University of Massachusetts Lowell.

10.1021/jp055324u CCC: $33.50
Published on Web 12/23/2005

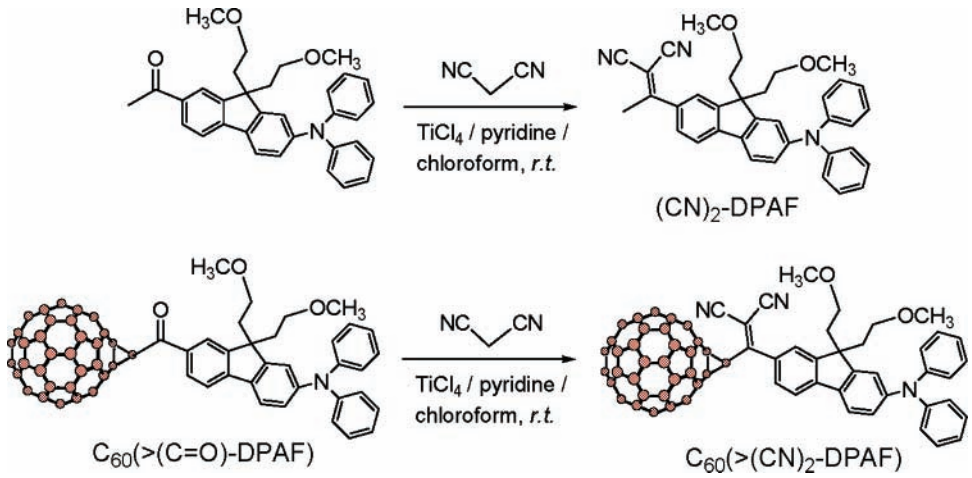

Figure 1. Molecular structures and synthetic procedures of $(CN)_2-$DPAF and $C_{60}(>(CN)_2-$DPAF).

mmol) were added under nitrogen atmosphere, followed by anhydrous chloroform (20 mL) to give a clear yellow solution. It was then added pyridine (320 mg, 4.0 mmol) and an excess amount of titanium tetrachloride (~3.0 mL) with continuous stirring. The reaction mixture turned immediately to deep brown. The solution was stirred for an additional 10 min and subsequently quenched with water (50 mL). The liquid was concentrated in a vacuum and purified using preparative thin-layer chromatography (silica gel) with a solvent mixture of hexane: ethyl acetate (3:2) as eluent. A chromatographic band at $R_f = 0.34$ was isolated to give $(CN)_2-$DPAF as bright yellow solids in 67% yield (400 mg).

Spectroscopic data of $(CN)_2-$DPAF: ^{1}H NMR (200 MHz, $CDCl_3$, ppm) δ 7.71−7.59 (m, 4H), 7.34−7.28 (m, 4H), 7.17−7.06 (m, 12H), 3.06 (s, 6H), 2.87−2.77 (m, 4H), 2.72 (s, 3H), and 2.33−2.19 (m, 4H); ^{13}C NMR (200 MHz, $CDCl_3$, ppm) δ 175.3, 151.9, 150.1, 149.6, 147.8, 146.8, 132.1, 132.2, 129.8, 127.9, 125.1, 124.6, 123.9, 123.2, 122.8, 122.0, 119.8, 118.3, 113.9, 113.7, 83.5, 68.9, 58.8, 52.1, 39.5, 30.1, and 24.5.

Synthesis of 7-(1,2-dihydro-1,2-methanofullerene[60]-61-{1,1-dicyanoethylene})-9,9-dimethoxyethyl-2-diphenylamino-fluorene $C_{60}(>(CN)_2-$DPAF). To a mixture of $C_{60}(>(C=O)-$DPAF) (500 mg, 0.04 mmol) and malononitrile (60 mg, 0.91 mmol) in anhydrous chloroform (75 mL) were added pyridine (131 mg, 1.6 mmol) and an excess amount of titanium tetrachloride (~1.0 mL) with continuous stirring under nitrogen atmosphere. This deep black blue solution was stirred for an additional 10 min and quenched with water (100 mL). The liquid was concentrated in a vacuum to give crude dark red solids, which were purified by column chromatography (silica gel) using chloroform as eluent. The product $C_{60}(>(CN)_2-$DPAF) at $R_f = 0.11$ was obtained as red solids in 63% yield (325 mg).

Spectroscopic data of $C_{60}(>(CN)_2-$DPAF): FT-IR (KBr) ν_{max} 3430, 2920, 2865, 2222, 1591, 1536, 1489, 1465, 1427, 1344, 1318, 1277, 1185, 1114, 821, 751, 697, 574, 525, and 480 cm^{-1}; UV−vis ($CHCl_3$) λ_{max} (ϵ) 255 (1.4×10^5), 322 (6.5×10^4), and 502 nm (2.4×10^4 L/mol/cm); ^{1}H NMR (500 MHz, $CDCl_3$, ppm) δ 8.18 (dd, $J = 8$ Hz, $J = 1.6$ Hz, 1H), 8.16 (d, $J = 1.6$ Hz, 1H), 7.82 (d, $J = 8$ Hz, 1H), 7.62 (d, $J = 8$ Hz, 1H), 7.33−7.28 (m, 4H), 7.16−7.13 (m, 5H), 7.12−7.07 (m, 3H), 5.57 (s, 1H), 3.01 (s, 6H), 2.78 (t, $J = 3$ Hz, 4H), and 2.38−2.24 (m, 4H); ^{13}C NMR (500 MHz, $CDCl_3$, ppm) δ 168.7, 152.3, 150.8, 150.1, 147.8, 147.7, 146.7, 146.3, 145.8, 145.7, 145.6, 145.3, 145.1, 144.9, 144.7, 144.2, 144.1, 143.5, 143.4, 143.4, 143.3, 142.9, 142.5, 142.4, 141.9, 141.5, 137.9, 137.5, 132.8, 129.9, 129.1, 125.3, 124.1, 123.4, 123.1, 122.4, 120.3, 118.1, 113.7, 113.6, 88.5, 72.9, 68.9, 58.9, 52.1, 41.7, and 39.8.

Instrumentation. Molecular orbital calculations were carried out by using Gaussian 98 (HF-6-21G* level). The cyclic voltammetry and differential pulse voltammetry measurements were performed on a BAS CV-50 W electrochemical analyzer in deaerated solution containing Bu_4NPF_6 (0.1 M) as a supporting electrolyte with a scan rate of 100 mV s^{-1}. The potentials were expressed vs ferrocene/ferrocenium (Fc/Fc^+) as an internal standard.

Steady-state absorption spectra were measured using an optical cell (0.2−1.0 cm) on a JASCO V-570 spectrophotometer. Steady-state fluorescence spectra were recorded on a Shimidzu RF-5300 PC spectrofluorophotometer equipped with a photomultiplier tube having high sensitivity up to 800 nm. Emission spectra of the singlet oxygen ($^1O_2$*) in the near-IR regions were detected by using an InGaAs detector.

Time-resolved fluorescence measurements were preformed by a single-photon counting method using second harmonic generation (SHG, 400 nm) of a Ti-sapphire laser (Spectra-Physics, Tsunami 3950-L2S, 1.5 ps fwhm) and a streakscope (Hamamatsu Photonics, C4334−01) equipped with a polychromator as an excitation source and a detector, respectively.[18] Nanosecond transient absorption spectra were measured using a laser light source at the excitation wavelength of 532 nm. In the near-IR region (600−1700 nm), a Ge avalanche photodiode module (Hmamatsu Photonics, C5331−SPL) was used as a detector for monitoring the light from a pulsed Xe flash lamp (Tokyo instruments, XF80−60). All the measurements were carried out at 23 °C using freshly prepared Ar-saturated solutions to eliminate the influence of O_2 effect.

Results and Discussion

Synthesis and Solubility. Both compounds $(CN)_2-$DPAF and $C_{60}(>(CN)_2-$DPAF) were synthesized from the corresponding keto-derivatives by the substitution reaction of malononitrile in the presence of $TiCl_4$, as shown in Figure 1. Both $(CN)_2-$DPAF and $C_{60}(>(CN)_2-$DPAF) are soluble in common organic solvents, such as toluene, anisole, *o*-dichlorobenzene, and PhCN, however, with less solubility for $C_{60}(>(CN)_2-$DPAF) in highly polar DMF.

Computational Studies. Computational studies were performed by using Hartree−Fock method at 6-21G(*) level to obtain insights on the molecular geometry and the electronic structure. Figure 2 shows the optimized structure of $(CN)_2-$DPAF, in which the 9-dimethoxyethyl groups were replace by the 9-ethyl for simplicity. The majority of the electron density of the highest occupied molecular orbital (HOMO) was found to be located on the DPAF moiety, whereas the lowest

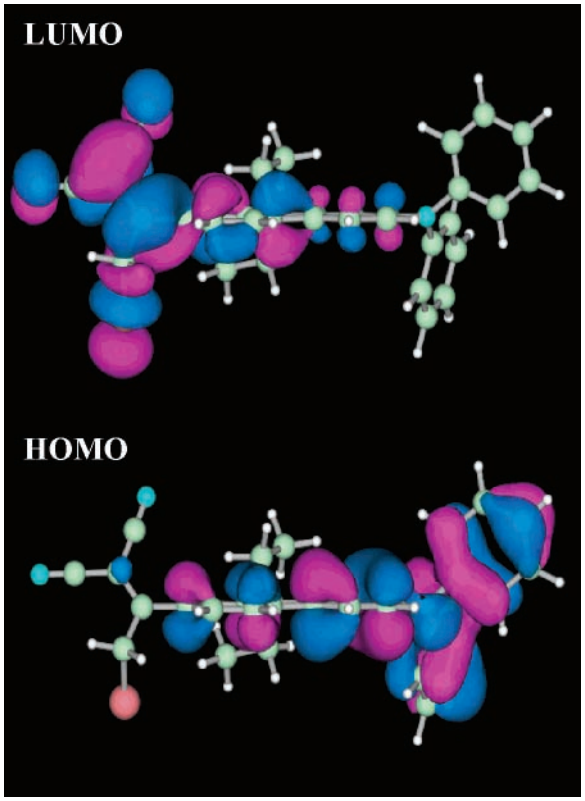

Figure 2. Optimized structure and the HOMO and LUMO of the diethyl-C_9 analogous of $(CN)_2$−DPAF calculated by HF(6-21G*) basis set.

unoccupied molecular orbital (LUMO) was located mainly on the >C═C(CN)$_2$ groups, spreading to one of the phenyl groups of the fluorene moiety. These MO's suggest that the charge-separated state is mainly attributed to $(CN)_2^{\bullet-}$−$DPAF^{\bullet+}$.

Figure 3 shows the optimized structure for C_{60}(>$(CN)_2$−DPAF). The center-to-center distance (R_{CC}) between C_{60} and DPAF moieties was found to be 12 Å. The majority of the electron density of HOMO was found to be delocalized over the DPAF moiety, whereas the LUMO located on the C_{60} spheroid, suggesting $C_{60}^{\bullet-}$(>$(CN)_2$−$DPAF^{\bullet+}$) as the most stable charge-separated state. The radii of ion radicals of DPAF (R^+) and C_{60} (R^-) were found to be 7.7 and 4.2 Å, respectively. In the LUMO+3 level, the electron density concentrates mainly on the >C═C(CN)$_2$ moiety, whereas the electron distributions of the LUMO+1 and LUMO+2 levels are almost the same as that of the LUMO.

Electrochemical Studies. Determination of the redox potentials in donor−acceptor systems is essential for the evaluation of the energetics of electron-transfer reactions. In the case of $(CN)_2$−DPAF in benzonitrile, the first oxidation potential (E_{ox}) of the DPAF moiety and the first reduction potential (E_{red}) of the >C═C(CN)$_2$ moiety were observed at +0.62 and −1.34 V vs Fc/Fc^+, respectively. Similar measurements of C_{60}(>$(CN)_2$−DPAF) showed the first E_{ox} value of the DPAF moiety and the first E_{red} value of the C_{60} moiety at 0.64 V and −0.76 V vs Fc/Fc^+, respectively, in benzonitrile. Driving forces for charge-recombination ($-\Delta G_{CR}$) and charge-separation ($-\Delta G_{CS}$) can be calculated based on the electrochemical data by eqs 1 and 2:[19]

$$-\Delta G_{CR} = E_{ox} - E_{red} - \Delta G_S \quad (1)$$

$$-\Delta G_{CS} = \Delta E_{0-0} - (-\Delta G_R) \quad (2)$$

Here, ΔE_{0-0} is defined as the energy of the 0−0 transition between the lowest excited state and ground state and determined from the fluorescence emission. The static energy (ΔG_S) was calculated as $-e^2/(4\pi\epsilon_0\epsilon_R R_{CC})$, in which the terms e, ϵ_0, and ϵ_R are defined as elementary charge, vacuum permittivity, and static dielectric constant of the solvent used in the rate and redox potential measurements, respectively. The values of $-\Delta G_{CS}$ and $-\Delta G_{CR}$ are listed in Tables 1 and 2. From the estimated $-\Delta G_{CS}$ values, the generations of $(CN)_2^{\bullet-}$−$DPAF^{\bullet+}$ and $C_{60}^{\bullet-}$(>$(CN)_2$−$DPAF^{\bullet+}$), via the excited CT state and $^1C_{60}$*, are exothermic in polar and less polar solvents. The charge-separation process, via the excited triplet state of C_{60} ($^3C_{60}$*), is sufficiently exothermic only in benzonitrile.

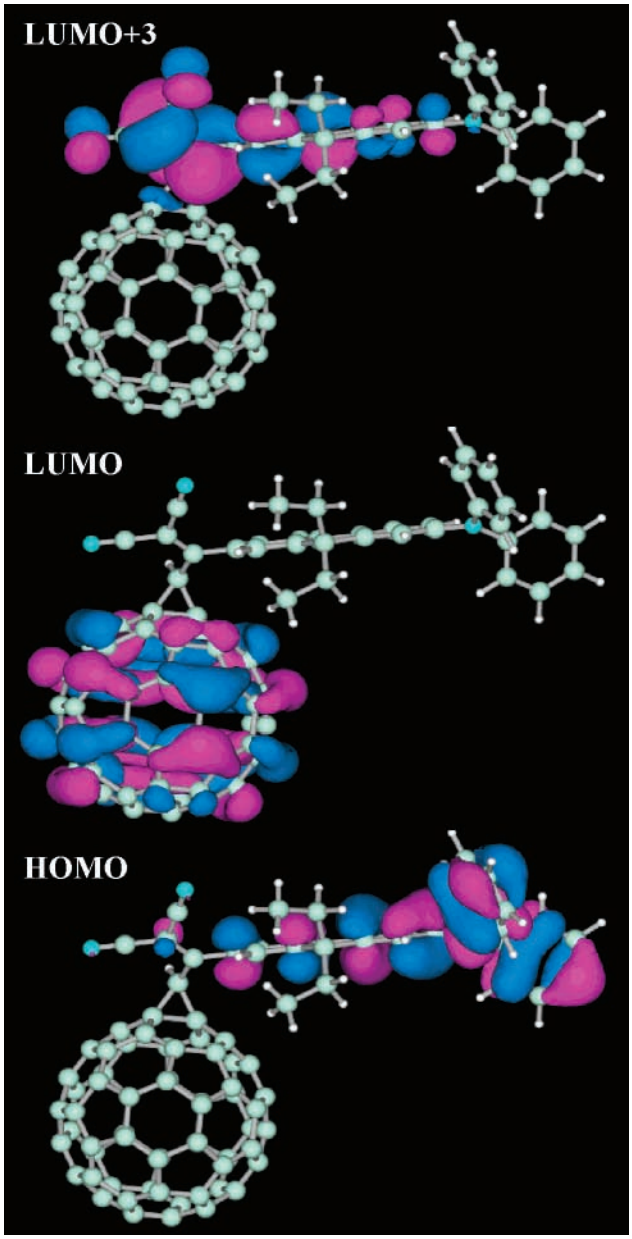

Figure 3. Optimized structure and the HOMO, LUMO, and LUMO+3 of the diethyl-C_9 analogous of C_{60}(>$(CN)_2$−DPAF) calculated by HF(6-21G*) basis set.

In a nonpolar solvent such as toluene, the energy level of the CS state is lower than that of ^{1}CT*, but higher than $^1C_{60}$* suggesting exothermic characteristics for the CS process from ^{1}CT* and endothermic from $^1C_{60}$*. However, the ΔG_{CS} value of the CS state in toluene may not be reliable since the Rehm−Weller model is oversimplified.

Steady-State Absorption Measurements. The absorption spectrum of DPAF displayed a band centered at 400 nm in the

TABLE 1: Free-Energy Changes ($-\Delta G_{CS}^{CT}$), Fluorescence Lifetimes (τ_f) Monitored at 600−700 nm, Rate Constants (k_q^{CT}), and Quantum Yields (Φ_q^{CT}) for Quenching Processes of the ^{1}CT* State of C_{60}(>$(CN)_2$−DPAF) in Different Solvents

solvent	$-\Delta G_{CS}^{CT}$/eV	τ_f/ps	k_q^{CT}/s^{-1}	Φ_q^{CT}
PhCN	1.08	50 (65%), 2000 (35%)	1.9×10^{10}	0.96
DCB	0.99	50 (70%), 2000 (30%)	1.9×10^{10}	0.96
ANS	0.75[a]	51 (70%), 2000 (30%)	1.8×10^{10}	0.91
toluene	0.42[a]	53 (70%), 2000 (30%)	1.7×10^{10}	0.90

[a] $\Delta G_S = e^2/(4\pi\Delta\epsilon_0)[(^1/_2R_+ + {}^1/_2R_- - 1/R_{CC})1/\epsilon_R - (^1/_2R_+ + {}^1/_2R_-)1/\epsilon_S]$, where ΔE_{0-0} is the energy of the CT transition of C_{60}(>$(CN)_2$−DPAF) (= 2.25 eV); ϵ_S refers to the dielectric constant of anisole and toluene.

TABLE 2: Free-Energy Changes ($-\Delta G_{CS}$), Fluorescence Lifetimes (τ_f), Rate Constants (k_{CS}^{C60}), and Quantum Yields (Φ_{CS}^{C60}) for Charge-Separation Processes of C_{60}(>$(CN)_2$−DPAF) via $^1C_{60}$* in Different Solvents

solvent	$-\Delta G_{CS}$/ eV	τ_f/ ps	k_{CS}^{C60}/ s^{-1}	Φ_{CS}^{C60}
PhCN	0.58	70 (70%) 2000 (30%)	1.3×10^{10}	0.94
DCB	0.49	170 (85%)	5.2×10^9	0.88
ANS	0.25	220 (85%)	3.9×10^9	0.85
toluene	−0.08	1400 (100%)		

visible region, as shown in Figure 4. In the case of $(CN)_2$−DPAF, a new band appeared at 430 nm, which was attributed to the CT transition from the DPAF to the C═C$(CN)_2$ moiety, corresponding to the transition from the HOMO level to the LUMO level of $(CN)_2$−DPAF as shown in Figure 2. Upon the addition of $FeCl_3$ as a strong oxidizing agent to the solution containing $(CN)_2$−DPAF, a new band appeared at 874 nm corresponding to the DPAF radical cation moiety (Supporting Information). When $(CN)_2$−DPAF is covalently bound with C_{60} in close vicinity, the C_{60} moiety influences the CT transition from the DPAF to C═C$(CN)_2$ moiety, showing a band red-shifted to 490 nm in the absorption spectrum of C_{60}(>$(CN)_2$−DPAF). This band is attributed to the transition from the HOMO level to the LUMO+3 level of C_{60}(>$(CN)_2$−DPAF) shown in Figure 3. Appreciable solvent polarity effect was found in the absorption spectra of $(CN)_2$−DPAF and C_{60}(>$(CN)_2$−DPAF) (Supporting Information).

Steady-State Fluorescence Measurement. Steady-state fluorescence spectra of DPAF, $(CN)_2$−DPAF, and C_{60}(>$(CN)_2$−

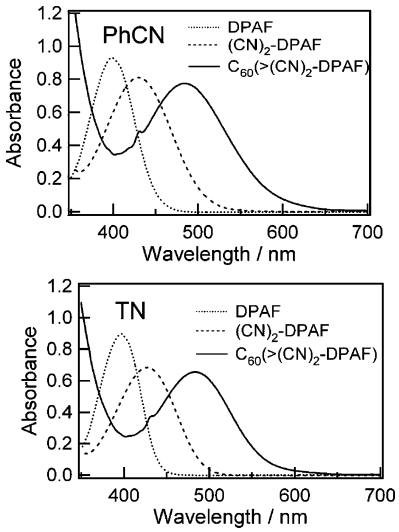

Figure 4. Steady-state absorption of DPAF, $(CN)_2$−DPAF, and C_{60}(>$(CN)_2$−DPAF) (upper panel) in PhCN and (lower panel) in toluene. The concentrations were maintained at 5 μM.

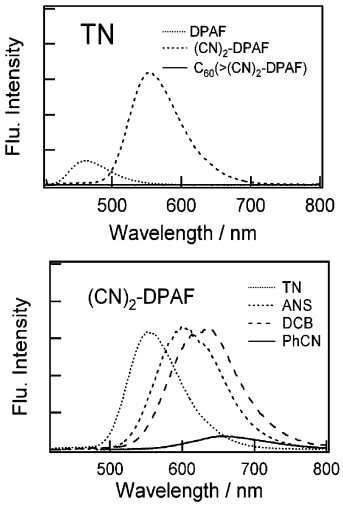

Figure 5. (Upper panel) Steady-state fluorescence spectra of DPAF, $(CN)_2$−DPAF, and C_{60}(>$(CN)_2$−DPAF) in toluene. (Lower panel) $(CN)_2$−DPAF in different solvents. The concentrations were maintained at 5 μM; λ_{ex} = 400 nm.

DPAF) were recorded in toluene by photoexcitation at 400 nm (Figure 5, upper panel). The spectrum of the basic DPAF unit showed a maximum of the fluorescence peak centered around 460 nm. Attachment of conjugative electron-withdrawing malononitrile onto DPAF forming $(CN)_2$−DPAF resulted in a large red-shift of the fluorescence peak to 560 nm in toluene and 660 nm in benzonitrile (Figure 5, lower panel). The red-shifted emission bands are characteristics of the CT excited state, $[(CN)_2^{\delta-}-DPAF^{\delta+}]$*, which is stabilized in polar solvents more than in nonpolar solvents. Furthermore, the shifts of emission peaks became more pronounced with the increase in solvent polarity than the corresponding shifts of absorption peaks, indicating a progressive increase of the dipole moment in the excited state.

In addition, a linear relationship was obtained between the energy of the CT emission and the solvent polarity parameter $\Delta f(\epsilon,n)$, according to eqs 3 and 4,[20−22]

$$\nu_{ex} = \nu_{ex}(0) - (2\mu_{ex}^2/4\pi\epsilon_0 hca^3)\,\Delta f \qquad (3)$$

$$\Delta f = (\epsilon_R - 1)/(2\epsilon_R + 1) - (n^2 - 1)/(2n^2 + 1) \qquad (4)$$

where ν_{ex} is the CT fluorescence maximum in a given solvent (in cm^{-1}), $\nu_{ex}(0)$ is defined as the maximum in vacuo, μ_{ex} is the dipole moment of the excited CT state, h is Planck's constant, c is the velocity of light in a vacuum, a is the radius of the solvent cavity (10 Å), and Δf is a parameter measuring the solvent polarity from ϵ_R and refractive index n (eq 4). Linear regression analysis of ν_{ex} against Δf on the basis of eq 3 leads to a slope of 1.96×10^4 (Supporting Information), from which μ_{ex} was estimated to be 13.7 D. The large dipole moment implies the high CT degree of $[(CN)_2^{\delta-}-DPAF^{\delta+}]$*.

In the case of C_{60}(>$(CN)_2$−DPAF), the emission arising from the corresponding absorption band at 490 nm was absent in toluene as shown in Figure 5 (upper panel). Similar fluorescence quenching of C_{60}(>$(CN)_2$−DPAF) was observed in benzonitrile (Supporting Information). As possible quenching pathways, the electron-transfer process from $C_{60}[>((CN)_2-DPAF)]^*_{CT}$ to $C_{60}^{\bullet-}(>(CN)_2-DPAF^{\bullet+})$ can be taken into account in addition to the energy-transfer process to the C_{60} moiety yielding $^1C_{60}$*(>$(CN)_2$−DPAF). The latter process should lead to a fluorescence peak of $^1C_{60}$* expected to appear at 710 nm. However, it was not readily visible owing to a very low

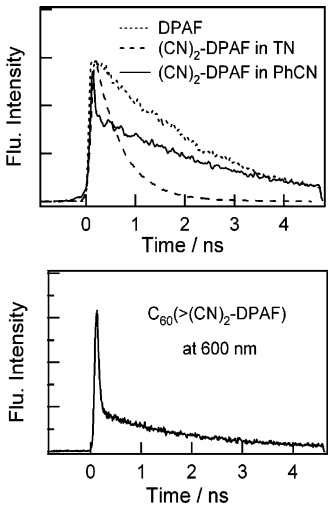

Figure 6. (Upper panel) Fluorescence decay profiles of DPAF, $(CN)_2$−DPAF in PhCN, and $(CN)_2$−DPAF in toluene monitored at 550 nm. (Lower panel) C_{60}(>$(CN)_2$−DPAF) monitored at 600 nm in toluene. The concentrations were maintained at 0.05 mM; $\lambda_{ex} = 400$ nm

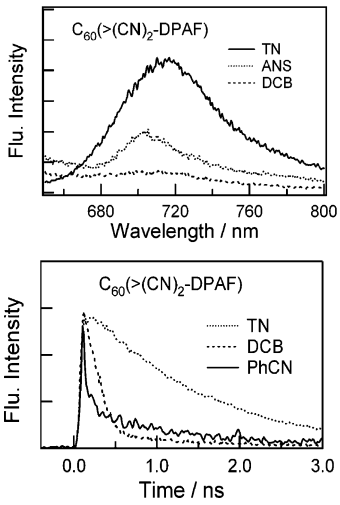

Figure 7. (Upper panel) Time-resolved fluorescence spectra of C_{60}(>$(CN)_2$−DPAF) in different solvents. (Lower panel) Fluorescence decay profiles of C_{60}(>$(CN)_2$−DPAF) monitored at 700 nm in PhCN, DCB, and toluene. The concentrations were maintained at 0.05 mM; $\lambda_{ex} = 400$ nm

fluorescence quantum yield (Φ_F) of $^1C_{60}$* in less than 0.0001.[3−5] To further understand the reaction mechanism and follow the kinetics of photoinduced processes, picosecond time-resolved emission studies were performed in the following section.

Fluorescence Lifetime Measurements. Fluorescence decay-time profiles of DPAF, $(CN)_2$−DPAF, and C_{60}(>$(CN)_2$−DPAF) were collected by applying 400 nm laser light (Figure 6, upper panel). As a result, the fluorescence time profile of DPAF at 460 nm exhibited a single-exponential decay with a lifetime (τ_f) of 2100 ps in either polar or nonpolar solvents. For the excited CT state of $(CN)_2$−DPAF, substantial quenching of the fluorescence lifetime was observed. In toluene, the fluorescence decay-time profile of $(CN)_2$−DPAF at 550 nm revealed a single-exponential decay with $\tau_f = 550$ ps. In PhCN, the fluorescence decay of $(CN)_2$−DPAF at 670 nm could be fitted satisfactorily by a biexponential decay; from the short lifetime component, the τ_f value was found to be 23 ps.

Similar measurements were performed on C_{60}(>$(CN)_2$−DPAF) sample. Resulting time profiles of the CT bands were monitored at 600 nm in both polar and nonpolar solvents by applying the 400 nm laser light. Decay-time profiles taken at 600 nm could be fitted satisfactorily with a biexponential decay. The major fast decay with τ_{sample} of about 53 ps in toluene is slightly longer than that in other polar solvents (Table 1). Fluorescence quenching of the ^{1}CT* state may involve the following: (1) the initial electron-transfer process to yield C_{60}(>$(CN)_2^{\bullet-}$−$DPAF^{\bullet+}$) followed by electron-shift to afford $C_{60}^{\bullet-}$(>$(CN)_2$−$DPAF^{\bullet+}$), (2) the direct electron-transfer process between the C_{60} and DPAF moieties to give $C_{60}^{\bullet-}$(>$(CN)_2$−$DPAF^{\bullet+}$), and (3) the energy-transfer process from the excited CT complex to yield the $^1C_{60}$* moiety, which decays via the CS process to form $C_{60}^{\bullet-}$(>$(CN)_2$−$DPAF^{\bullet+}$).

The fluorescence quenching rate (k_q^{CT}) and quantum yield (Φ_q^{CT}) via the ^{1}CT* state were calculated by using eqs 5 and 6, in which the fluorescence lifetime of $(CN)_2$−DPAF in toluene was employed as $\tau_{reference}$. The evaluated k_q^{CT} and Φ_q^{CT} are listed in Table 1.

$$k_q^{CT} = (\tau_{sample})^{-1} - (\tau_{reference})^{-1} \quad (5)$$

$$\Phi_q^{CT} = k_q^{CT}/(\tau_{sample})^{-1} \quad (6)$$

The k_q^{CT} values were evaluated to be $(1.7-1.9) \times 10^{10}$ s^{-1} in all solvents. The fact of k_q^{CT} values independent of the solvent polarity reveals the dominance of the energy transfer process in yielding $^1C_{60}$*. It is plausible since the energy-transfer rates depend mainly on the reflective index, which is almost the same among the solvents employed in the present study. The slightly higher k_q^{CT} values in polar solvents than that in toluene suggest the charge-separation process taking place competitively to the energy-transfer process.

By scanning the emission wavelength of C_{60}(>$(CN)_2$−DPAF) to longer wavelength regions (700−800 nm), the emission band of $^1C_{60}$* at 720 nm appeared after considerable quenching of the ^{1}CT* state (Figure 7, upper panel) in nonpolar and less polar solvents. This finding suggests the population mechanism of the $^1C_{60}$* state involving the energy process since the direct excitation of the C_{60} moiety to $^1C_{60}$* is unlikely to occur with the 400 nm light excitation. The fluorescence intensity of $^1C_{60}$* was significantly quenched by increasing the solvent polarity that led to a nearly invisible, weak fluorescence intensity of $^1C_{60}$* in benzonitrile. Fluorescence decay-time profiles of $^1C_{60}$*(>$(CN)_2$−DPAF) in various solvents are shown in Figure 7 (lower panel). The time profile in toluene exhibited a single-exponential decay with a lifetime of 1300 ps which is the same as that of the C_{60} reference,[1−5,12,16] suggesting that the charge-separation process does not take place via the $^1C_{60}$* moiety in nonpolar solvent. This conclusion is also supported by the positive $\Delta G_{CS}^{C_{60}}$ value in toluene as listed in Table 2. In more polar solvents, short fluorescence lifetimes of the $^1C_{60}$* moiety of C_{60}(>$(CN)_2$−DPAF) were observed that revealed the concurrence of charge-separation processes taking place via the $^1C_{60}$* moiety in polar solvents, in agreement with the negative $\Delta G_{CS}^{C_{60}}$ values. Thus, the charge-separation rate constant ($k_{CS}^{C_{60}}$) and quantum yield ($\Phi_{CS}^{C_{60}}$) for the generation of $C_{60}^{\bullet-}$(>$(CN)_2$−$DPAF^{\bullet+}$) can be evaluated by using eqs 5 and 6, where the lifetime of the $^1C_{60*}$ moiety in toluene was employed as $\tau_{reference}$. The $k_{CS}^{C_{60}}$ and $\Phi_{CS}^{C_{60}}$ values were estimated as listed in Table 2.

Nanosecond Transient Spectroscopic Measurements. The nanosecond transient absorption technique was utilized to confirm the generation of charge-separated states of C_{60}(>$(CN)_2$−DPAF) and monitor their charge-recombination processes in various solvents.

Transient absorption spectra of C_{60}(>$(CN)_2$−DPAF) in Ar-saturated toluene (Figure 8, upper panel) displayed a broad peak centered at 720 nm, which is attributed to the $^3C_{60}$* moiety.[23]

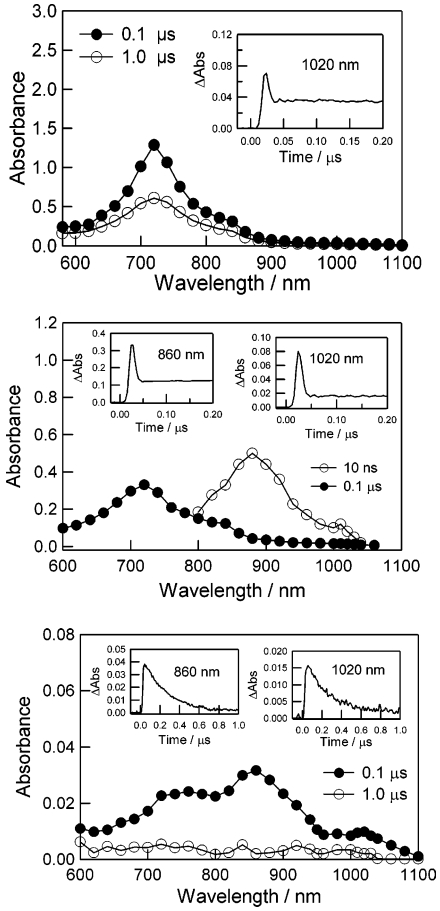

Figure 8. Transient absorption spectra obtained by 532 nm laser light of $C_{60}(>(CN)_2-DPAF)$ (0.07 mM) in Ar-saturated toluene (upper panel), DCB (middle panel), and PhCN (lower panel). Inset: time profiles at 860 and 1020 nm.

Its formation might be rational based on following plausible mechanisms involving: (1) the energy transfer process from the $^1CT^*$ state to yield $^1C_{60}^*$, followed by the intersystem crossing to give $^3C_{60}^*$ or (2) the CS process via the $^1CT^*$ state to yield $C_{60}^{\bullet-}(>(CN)_2-DPAF^{\bullet+})$. The latter mechanism was supported by the detection of quick rise-decay time profiles taken at 860 and 1020 nm. In this process, the resulting $C_{60}^{\bullet-}(>(CN)_2-DPAF^{\bullet+})$ further decayed to the $^1C_{60}^*$ moiety with a rate constant of $1.5 \times 10^8\ s^{-1}$ and subsequently followed by the relaxation of $^1C_{60}^*$ to the corresponding $^3C_{60}^*$ moiety. This is consistent with the observation of almost unquenchable fluorescence of the $^1C_{60}^*$ moiety in toluene.

In *o*-dichlorobenzene and anisole, the transient spectrum of $C_{60}(>(CN)_2-DPAF)$ (Figure 8, middle panel) taken at a 10 ns time scale showed two characteristic bands of $C_{60}^{\bullet-}$ and $DPAF^{\bullet+}$ at 1020 and 860 nm, respectively. Time-profiles of these radical ion pairs indicated fast rise kinetics in a time scale shorter than 10 ns that can be attributed to the occurrence of CS processes via the $^1C_{60}^*$ moiety and/or the $^1CT^*$ moiety. Judging from the energy level of the CS states in *o*-dichlorobenzene and anisole, such electron transfer is thermodynamically favorable via $^1CT^*$ and $^1C_{60}^*$ and leads to the CS state. On the other hand, the initial quick decay within 20 ns is attributed to the subsequent CR process. The absorption profile, showing the band maximum centered at 720 nm, detected at 0.1 μs can be correlated with the $^3C_{60}^*$ moiety.

In the case of benzonitrile, the transient absorption spectrum depicted at 100 ns revealed characteristic bands of the radical ion pair at 860 and 1020 nm with a weak transient band of the $^3C_{60}^*$ moiety at 700 nm. These characteristic bands arising from the $DPAF^{\bullet+}$ and $C_{60}^{\bullet-}$ moieties were employed to determine the rate constants of the charge recombination process (k_{CR}), since the decays were well fitted by a single-exponential. From the k_{CR} values, the lifetimes of the radical ion pairs (τ_{RIP}) were calculated as listed in Table 3. In benzonitrile, the lifetime of $C_{60}^{\bullet-}(>(CN)_2-DPAF^{\bullet+})$ was evaluated to be 270 ns at room temperature. The value of τ_{RIP} in benzonitrile is significantly longer than those obtained in *o*-dichlorobenzene and anisole. This can be reasonably interpreted by the following: (1) stabilization of the radical ion pairs with increasing polarity of the solvent and (2) the triplet-spin state character of the ion-pair radicals.[11]

TABLE 3: Free-Energy Changes (ΔG_{CR}), Rate Constants (k_{CR}), and Lifetimes for the Radical Ion Pairs (τ_{RIP}) of $C_{60}^{\bullet-}(>(CN)_2-DPAF^{\bullet+})$ in Different Solvents

solvent	ΔG_{CR}/eV	k_{CR}/s^{-1}	τ_{RIP}/ns
PhCN	1.17	3.7×10^6	270
DCB	1.26	1.5×10^8	7
ANS	1.50	1.5×10^8	7
toluene	1.83		

Singlet Oxygen Generation in Toluene. Predominant generation of the $^3C_{60}^*$ moiety as detected upon the laser excitation (532 nm) of the CT band of $C_{60}(>(CN)_2-DPAF)$ in toluene prompted us to investigate the photosensitized production of the singlet oxygen state ($^1O_2^*$) by the addition of molecular oxygen. Successful detection of $^1O_2^*$ may allow its correlation to important photochemical processes involved in the chemical, biological, and medical sciences. A considerable increase in the decay rate of $^3C_{60}^*(>(CN)_2-DPAF)$ at 700 nm was observed in the presence of O_2, suggesting its effective quenching of the $^3C_{60}^*$ moiety. On the basis of the pseudo-first-order plot, the triplet quenching rate constant by O_2 (k_{O_2}) was calculated to be $1.6 \times 10^9\ M^{-1}\ s^{-1}$, which is slightly smaller than the diffusion-controlled-limit ($9 \times 10^9\ M^{-1}\ s^{-1}$ in toluene).[25] During the quenching process of $^3C_{60}^*$ by O_2, intermolecular triplet energy transfer yielding $^1O_2^*$ was substantiated by observing its fluorescence emission at 1270 nm, as shown in Figure 9. The yield of $^1O_2^*$ via $^3C_{60}^*(>(CN)_2-DPAF)$ was nearly identical to that of the pristine $^3C_{60}^*$, confirming the occurrence of energy transfer from the $^1CT^*$ state to the C_{60} moiety, followed by the intersystem crossing toward the formation of $^3C_{60}^*(>(CN)_2-DPAF)$.

Energy Diagram. On the basis of thermodynamic data, the energy diagram of photoinduced processes of $C_{60}(>(CN)_2-DPAF)$ was elucidated as shown in Figure 10. By exciting the CT complex, there are many possible quenching pathways of $[C_{60}^{\delta-}(>(CN)_2-DPAF^{\delta+})]^*_{CT}$ including the following: (1) the transformation from the $^1CT^*$ state to fully charge-separated state yielding $C_{60}(>(CN)_2^{\bullet-}-DPAF^{\bullet+})$, (2) the exothermic electron-shift process from the $C{=}(CN)_2$ moiety to the C_{60}

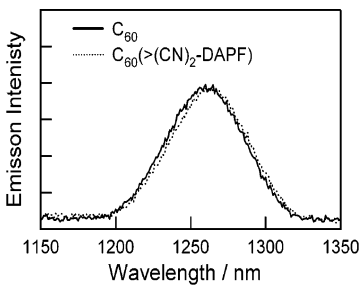

Figure 9. Emission spectra of $^1O_2^*$ in the near-IR region observed by the laser irradiation of C_{60} and $C_{60}(>(CN)_2-DPAF)$ in O_2-saturated toluene.

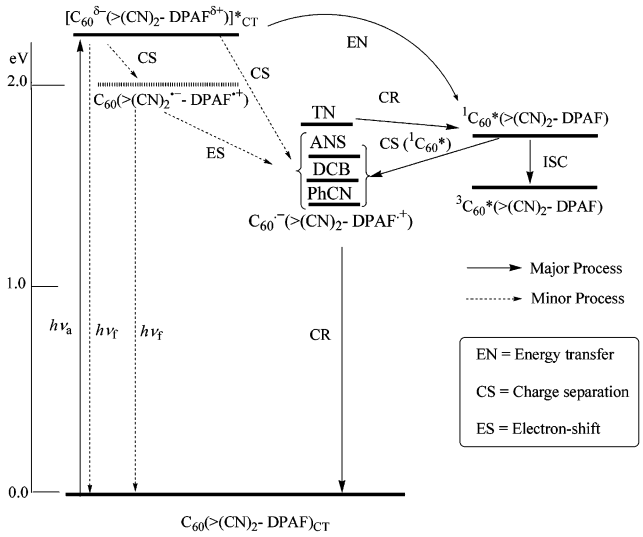

Figure 10. Energy diagrams for photochemical events of C_{60}(>$(CN)_2$−DPAF) in different organic solvents.

moiety, generating $C_{60}^{\bullet-}$(>$(CN)_2$−$DPAF^{\bullet+}$) although this process may be too fast to be observed in the present study, (3) the direct electron-transfer yielding $C_{60}^{\bullet-}$(>$(CN)_2$−$DPAF^{\bullet+}$), and (4) the energy-transfer process from the ^{1}CT* state to the C_{60} moiety yielding $^1C_{60}$*, which decayed by a charge separation process to yield $C_{60}^{\bullet-}$(>$(CN)_2$−$DPAF^{\bullet+}$).

Population of $^1C_{60}$*(>$CN)_2$−DPAF), produced by energy transfer from the ^{1}CT* state, is the main event concerned in toluene. The $^1C_{60}$*(>$CN)_2$−DPAF) state can be generated by the fast CR process of $C_{60}^{\bullet-}$(>$(CN)_2$−$DPAF^{\bullet+}$) following prior fast CS process, according to the observed fast rise in fluorescence intensity within 100 ps (Figure 7). These $^1C_{60}$*(>$(CN)_2$−DPAF) transient states decayed to populate the $^3C_{60}$* moiety by an intersystem crossing process. Afterward, efficient generation of $^1O_2$* from the $^3C_{60}$* moiety was realized.

In polar solvents, intramolecular energy transfer to the C_{60} moiety yielding $^1C_{60}$*(>$CN)_2$−DPAF) takes place competitively with the CS process from the ^{1}CT* state, as confirmed by the rapid fluorescence decay of ^{1}CT*. Subsequent CS process of $^1C_{60}$*(>$CN)_2$−DPAF) becomes a dominant course to yield the corresponding $C_{60}^{\bullet-}$(>$(CN)_2$−$DPAF^{\bullet+}$) which decays to the ground state via the CR process.

Charge-recombination process of $C_{60}^{\bullet-}$(>$(CN)_2$−$DPAF^{\bullet+}$) is apparently exothermic with favorable energy of more than 1.17 eV, suggesting that the CR process belongs to the inverted region of the Marcus parabola.[17,27] In benzonitrile, the τ_{RIP} value was found to be as long as 270 ns. That supports the inverted region based on the reorganization energies of fullerene dyads being considerably less than 0.6−0.7 eV. In *o*-dichlorobenzene and anisole, the τ_{RIP} values were found to be shorter than 10 ns, although the CR processes in these solvents belong to the deeper inverted region. As one of rationales, charge-recombination process in less polar solvents tends to occur prior to the full solvation of $C_{60}^{\bullet-}$(>$(CN)_2$−$DPAF^{\bullet+}$).

Conclusion

We report the photophysical properties of a methano[60]-fullerene derivative C_{60}(>$(CN)_2$−DPAF), consisting of a covalently bound C_{60} with diphenylaminofluorene (DPAF) via a bridging dicyanoethylene group. Strong electron-withdrawing characteristics of dicyanoethylenyl unit stimulated a strong charge-transfer (CT) band of the $(CN)_2$−DPAF moiety. Characters of subsequent processes induced by the excitation of the CT complex were significantly different from the corresponding C_{60} excitation. Deriving from the excited CT state, both charge-separation and energy-transfer processes took place competitively. Following energy transfer, the indirect charge separation process via $^1C_{60}$*(>$CN)_2$−DPAF) occurred in polar solvents, but not in nonpolar solvents.

In polar solvents, the fluorescence quenching step was associated with a rapid photoinduced electron-transfer pathway leading to the formation of radical ion pairs, detected by transient absorption spectroscopy. The lifetimes τ_{RIP} of $C_{60}^{\bullet-}$(>$(CN)_2$−$DPAF^{\bullet+}$) were evaluated to be 270 ns in benzonitrile and 7 ns in *o*-dichlorobenzene and anisole. Importantly, the observed data demonstrated the relatively long lifetime of $C_{60}^{\bullet-}$(>$(CN)_2$−$DPAF^{\bullet+}$) as compared with the previously reported value of C_{60}(>(C═O)−DPAF) (<20 ns in PhCN).[16] Such a comparatively long lifetime might be attributed to the small reorganization energy of the system associated with the essential contribution of dicyanoethylenyl groups as electron mediating subunits exceeding that of keto group. The observed data also substantiated the efficient photosensitizing generation of $^1O_2$* via $^3C_{60}$*(>$(CN)_2$−DPAF) as an important mechanism in the field of photodynamic therapy.

Acknowledgment. The present work was partly supported by a Grant-in-Aid on Scientific Research of Priority Aria (417) from the Ministry of Education, Science, Sports, and Culture of Japan. M.E.E.-K. is grateful for financial support by the JSPS Fellowship. We also thank the Air Force Office of Scientific Research under Contract Nos. FA9550-05-1-0154 and FA5209-04-P-0540 (Asian Office of Aerospace Research and Development) for financial support.

Supporting Information Available: Figure S1, absorbance of $(CN)_2$−DPAF (5×10^{-6} M) in the presence and absence of $FeCl_3$ (0.1 M) in DCB, Figure S2, steady-state absorption spectra of $(CN)_2$−DPAF in different solvents, Figure S3, steady-state absorption spectra of C_{60}(>$(CN)_2$−DPAF) in different solvents, Figure S4, relation between ν_{ex} and $f(\epsilon,n)$ for $(CN)_2$−DPAF in different solvents, Figure S5, steady-state fluorescence spectra of DPAF, $(CN)_2$−DPAF, and C_{60}(>$(CN)_2$−DPAF) in PhCN, and Figure S6, fluorescence decay profiles of C_{60}(>$(CN)_2$−DPAF) monitored at 600 nm in PhCN. This material is available free of charge via the Internet at http://pubs.acs.org.

References and Notes

(1) (a) Gust, D.; Moore, T. A. *Science* **1989**, *244*, 35. (b) Gust, D.; Moore, T. A. *Top. Curr. Chem.* **1991**, *159*, 103. (c) Wasielewski, M. R. *Chem. Rev.* **1992**, *92*, 435. (d) Paddon-Row: M. N. *Acc. Chem. Res.* **1994**, *27*, 18. (e) Sutin, N. *Acc. Chem. Res.* **1983**, *15*, 275. (f) Bard, A. J.; Fox, M. A. *Acc. Chem. Res.* **1995**, *28*, 141. (g) Piotrowiak, P. *Chem. Soc. Rev.* **1999**, *28*, 143.

(2) (a) *Introduction of Molecular Electronics*; Petty, M. C., Bryce, M. R., Bloor, D., Eds.; Oxford University Press: New York, 1995. (b) Ward, M. W. *Chem. Soc. Rev.* **1997**, *26*, 365 (c) Feldheim, D. L.; Keating, C. D. *Chem. Soc. Rev.* **1998**, *27*, 1. (d) Guldi, D. M.; Kamat, P. V. *Fullerenes, Chemistry, Physics and Technology*; Kadish, K. M., Ruoff, R. S., Eds.; Wiley-Interscience: New York, **2000**, pp 225−281.

(3) (a) Imahori, H.; Sakata, Y. *Eur. J. Org. Chem.* **1999**, 2445. (b) Meijer, M. D.; van Klink, G. P. M.; van Koten, G. *Coord. Chem. Rev.* **2002**, *230*, 141. (c) Bracher, P. J.; Schuster, D. I. Electron Transfer in Functionalized Fullerenes. In *Fullerenes: From Synthesis to Optoelectronic Properties*; Guldi, D. M., Martin, N., Eds.; Kluwer Academic Publishers: Norwell, MA; **2002**, pp 163-212. (d) Fujutsuka, M.; Ito, O. Photochemistry of Fullerenes. In *Handbook of Photochemistry and Photobiology*; Nalwa, H. S., Eds.; 2003; Vol. 2, Organic Photochemistry, pp 111−145.

(4) (a) Khan, S. I.; Oliver, A. M.; Paddon-Row: M. N.; Rubin, Y. *J. Am. Chem. Soc.* **1993**, *115*, 4919. (b) Williams, R. M.; Zwier, J. M.; Verhoeven, J. W. *J. Am. Chem. Soc.* **1995**, *117*, 4093. (c) Imahori, H.; Hagiwara, K.; Aoki, M.; Akiyama, T.; Taniguchi, S.; Okada, T.; Shirakawa, M.; Sakata, Y. *J. Am. Chem. Soc.* **1996**, *118*, 11771. (d) Guldi, D. M.;

Maggini, M.; Scorrano, G.; Prato, M. *J. Am. Chem. Soc.* **1997**, *119*, 974. (e) Liddell, P. A.; Kuciauska, D.; Sumida, J. P.; Nash, B.; Nguyen, D.; Moore, A. L.; Moore, T. A.; Gust, D. *J. Am. Chem. Soc.* **1997**, *119*, 1400.

(5) (a) Martin, N.; Schanez, L.; Illescas, B.; Perez, I. *Chem. Rev.* **1998**, *98*, 2527. (b) Imahori, H.; Yamada, H.; Guldi, D. M.; Endo, Y.; Shimomura, A.; Kundu, S.; Yamada, K.; Okada, T.; Sakata, Y.; Fukuzumi, S. *Angew. Chem., Int. Ed.* **2002**, *41*, 2344. (c) Guldi, D. M.; Fukuzmi, S. The Small Reorganization Energy of Fullerenes. In *Fullerenes: From Synthesis to Optoelectronic Properties*; Guldi, D. M., Martin, N., Eds.; Kluwer Academic Publishers: Norwell, MA; 2002; pp 237−265. (d) Fukuzumi, S.; Ohkubo, K.; Imahori, H.; Guldi, D. M. *Chem.*−*Eur. J.* **2003**, *9*, 1585.

(6) (a) Jiang, X.; Liu, M. S.; Jen, A. K.-Y. *J. Appl. Phys.* **2002**, *91*, 10147. (b) Belfield, K. D.; Bondar, M. V.; Morales, A. R.; Yavus, O.; Przhonska, O. V. *J. Phys. Org. Chem.* **2003**, *16*, 194. (c) Sung, H.-H.; Lin, H.-C. *Macromolecules* **2004**, *37*, 7945. (d) Feng, L.; Chen, Z.; Bai, F. *Spectrochim. Acta, Part A* **2004**, *60*, 3029.

(7) (a) Kraft, A.; Grimsdale, A. C.; Holmes, A. B. *Angew. Chem., Int. Ed.* **1998**, *37*, 402. (b) Bernius, M. T.; Inbasekaran, M.; O'Brien, J.; Wu, W. *Adv. Mater.* **2000**, *12*, 1737. (c) Tao, Y.-T.; Ko, C.-W. *U.S. Pat. Appl. Publ.* **2002**, 7. (d) Ego, C.; Grimsdale, A. C.; Uckert, F.; Yu, G.; Srdanov, G.; Mullen, K. *Adv. Mater.* **2002**, *14*, 809. (e) Svensson, M.; Zhang, F.; Veenstra, S. C.; Verhees, W. J. H.; Hummelen, J. C.; Kroon, J. M.; Inganas, O.; Anderrson, M. R. *Adv. Mater.* **200**3, *15*, 988. (f) Wang, X.; Perzon, E.; Delgado, J. L.; Cruz, P.; Zhang, D.-L.; Langa, F.; Anderson, M.; Inganas, O. *Appl. Phys. Lett.* **2004**, *85*, 5081.

(8) Saainova, D.; Miteva, T.; Nothefer, H.-G.; Scherf, U.; Glowacki, I.; Ulanski, J.; Fujikawa, H.; Neher, D. *Appl. Phys. Lett.* **2000**, *76*, 1810.

(9) (a) Williams, R. M.; Zwier, J. M.; Verhoeven, J. W. *J. Am. Chem. Soc.* **1995**, *117*, 4093. (b) Williams, R. M.; Koeberg, M.; Lawson, J. M.; An, Y.-Z.; Rubin, Y.; Paddon-Row: M. N.; Verhoeven, J. W. *J. Org. Chem.* **1996**, *61*, 5055. (c) Thomas, K. G.; Biju, V.; George, M. V.; Guldi, D. M.; Kamat, P. V. *J. Phys. Chem. A* **1998**, *102*, 5341. (d) Thomas, K. G.; Biju, V.; Guldi, D. M.; Kamat, P. V.; George, M. V. *J. Phys. Chem. B* **1999**, *103*, 8864. (e) Thomas, K. G.; Biju, V.; Guldi, D. M.; Kamat, P. V.; George, M. V. *J. Phys. Chem. A* **1999**, *103*, 10755.

(10) (a) Komamine, S.; Fujitsuka, M.; Ito, O.; Moriwaki, K.; Miyata, T.; Ohno, T. *J. Phys. Chem. A* **2000**, *104*, 11497. (b) Rajkumar, A. G.; Sandanayaka, S. D. A.; Ikeshita, K.; Itou, M.; Araki, Y.; Furusho, Y.; Kihara, N.; Ito, O.; Takata, T. *J. Phys. Chem. A* **2005**, *109*, 2428. (c) Sandanayaka, S. D. A.; Sasabe, H.; Araki, Y.; Furusho, Y.; Ito, O.; Takata, T. *J. Phys. Chem.* A **2004**, *108*, 5145.

(11) Yamanaka, K.; Fujitsuka, M.; Araki, Y.; Ito, O.; Aoshima, T.; Fukushima, T.; Miyashi, T. *J. Phys. Chem. A.* **2004**, *108*, 250.

(12) (a) Arbogast, J. W.; Foote, C. S.; Kao, M. *J. Am. Chem. Soc.* **1992**, *114*, 2277. (b) Biczok, L.; Linschitz, H. *Chem. Phys. Lett.* **1992**, *195*, 339. (c) Nonell, S.; Arbogast, J. W.; Foote, C. S. *J. Phys. Chem.* **1992**, *96*, 4169. (d) Steren, C. A.; von Willigen, H.; Biczok, L.; Gupta, N.; Linschitz, H. *J. Phys. Chem.* **1996**, *100*, 8920.

(13) (a) Komamine, S.; Fujitsuka, M.; Ito, O.; Itaya, A. *J. Photochem., Photobiol. A: Chem.* **2000**, *135*, 111. (b) Ito, O.; Sasaki, Y.; Yoshikawa, Y.; Watanabe. A. *J. Phys. Chem.* **1995**, *99*, 9838. (c) Ito, O. *Res. Chem. Intermed.* **1997**, *23*, 389. (d) Yahata, Y.; Sasaki, Y.; Fujitsuka, M.; Ito, O. *J. Photosci.* **1999**, *6*, 117.

(14) (a) Ghosh, H. N.; Palit, D. K.; Sapre, A. V.; Mittal, J. P. *Chem. Phys. Lett.* **1997**, *265*, 365. (b) Sension, R. J.; Szarka, A. Z.; Smith, G. R.; Hochstrasser, R. M. *Chem. Phys. Lett.* **1991**, *185*, 179.

(15) (a) Chiang, L. Y.; Padmawar, P. A.; Canteewala, T.; Tan, L.-S.; He, G. S.; Kanna, R.; Vaia, R.; Lin, T.-C.; Zheng, Q.; Prasad, P. N. *Chem. Commun.* **2002**, 1854. (b) Padmawar, P. A.; Canteenwala, T.; Verma, S.; Tan, L.-S.; Chiang, L. Y. *J. Macromol. Sci. A Pure Appl. Chem.* **2004**, *41*, 1387. (c) Padmawar, P. A.; Canteenwala, T.; Verma, S.; Tan, L.-S.; He, G. S.; Prasad, P. N.; Chiang, L. Y. *Synth. Met.* **2005**, *154*, 185.

(16) Luo, H.; Fujitsuka, M.; Araki, Y.; Ito, O.; Padmawar, P A.; Chiang, L. Y. *J. Phys. Chem. B* **2003**, *107*, 9312.

(17) (a) Marcus, R. A. *J. Chem. Phys.* **1956**, *24*, 966. (b) Marcus, R. A. *J. Chem. Phys.* **1957**, *26*, 867. (c) Marcus, R. A. *J. Chem. Phys.* **1957**, *26*, 872. (d) Marcus, R. A. *J. Chem. Phys.* **1965**, *43*, 679. (e) Marcus, R. A.; Sutin, N. *Biochim. Biophys. Acta* **1985**, *811*, 265.

(18) (a) Fujitsuka, M.; Ito, O.; Yamashiro, T.; Aso, Y.; Otsubo, T. *J. Phys. Chem. A* **2000**, *104*, 4876. (b) Fujitsuka, M.; Masuhara, A.; Kasai, H.; Oikawa, H.; Nakanishi, H.; Ito, O.; Yamashiro, Y.; Aso, Y.; Otsubo, T. *J. Phys. Chem. B* **2001**, *105*, 9930.

(19) Rehm, D.; Weller, A. *Isr. J. Chem.* **1970**, *8*, 259.

(20) Park, S. M.; Bard, A. J. *J. Am. Chem. Soc.* **1975**, *97*, 2978.

(21) Kavarnos, G. J.; Turro, N. J. *Chem. Rev.* **1986**, *86*, 401.

(22) (a) Maslak, P. *In Topics in Current Chemistry*; Mattay, J., Ed.; Springer-Verlag: Berlin, 1993; Vol. 168; Chapter 1. (b) Rath, M. C.; Mukherjee, T. *J. Phys. Chem. A* **1999**, *103*, 4993. (c) Wouter, V.; Viaene, L.; van der Auweraer, M.; De Schryver, F. C.; Masuhara, H.; Pansu, R.; Faure, J. *J. Phys. Chem. A* **1997**, *101*, 8157.

(23) (a) Guldi, D. M. *Chem. Commun.* **2000**, 321. (b) Reed, C. A.; Bolskar, R. D. *Chem. Rev.* **2000**, *100*, 1075. (c) Gust, D.; Moore, T. A.; Moore, A. L. *J. Photochem. Photobiol. B* **2000**, *58*, 63. (d) Imahori, H.; El-Khouly, M. E.; Fujitsuka, M.; Ito, O.; Sakata, Y.; Fukuzumi, S. *J. Phys. Chem. A.* **2001**, *105*, 325. (e) Imahori, H.; Guldi, D. M.; Tamaki, K.; Yoshida, Y.; Luo, C.; Sakata, Y.; Fukuzumi, S. *J. Am. Chem. Soc.* **2001**, *123*, 6617. (f) D'Souza, F.; Deviprasad, G. R.; El-Khouly, M. E.; Fujitsuka, M.; Ito, O. *J. Am. Chem. Soc.* **2001**, *123*, 5277.

(24) (a) El-Khouly, M. E.; Fujitsuka, M.; Ito, O. *J. Porphyrin Phthalocyanines* **2000**, *4*, 591. (b) Anderson, J. L.; An, Y.-Z.; Rubin, Y.; Foote, C. S. *J. Am. Chem. Soc.* **1994**, *116*, 9763. (c) Guldi, D. M.; Neta, P.; Asums, K.-D. *J. Phys. Chem.* **1994**, *98*, 4617. (d) Alam, M. M.; Watanabe, A.; Ito, O. *Bull. Chem. Soc. Jpn.* **1997**, *70*, 1833.

(25) (a) Smirnov, S. N.; Liddell, P. A.; Valssiouk, I. V.; Teslja, A.; Kuciauskas, D.; Braun, C. L.; Moore, A. L.; Moore, T. A.; Gust, D. *J. Phys. Chem. A* **2003**, *107*, 7567. (b) Montforts, F.-P.; Vlassiouk, I.; Smirnov, S.; Wedel, M. *J. Porphyrins Phthalocyanines* **2003**, *7*, 651. (c) Watanabe, N.; Kihara, N.; Fuirusho, Y.; Takata, T.; Araki, Y.; Ito, O. *Angew. Chem., Int. Ed.* **2003**, *42*, 681. (d) Guldi, D. M.; Hirsch, A.; Scheloske, M.; Dietel, E.; Troisi, A.; Zerbetto, F.; Prato, M. *Chem.*−*Eur. J.* **2003**, *9*, 4968. (e) El-Khouly, M. E.; Ito, O.; Smith, P. M.; D'Souza, F. *J. Photochem. Photobiol. C: Rev.* **2004**, *5*, 79. (f) Sutton, L. R.; Scheloske, M.; Pirner, K. S.; Hirsch, A.; Guldi, D. M.; Gisselbrecht, J.-P. *J. Am. Chem. Soc.* **2004**, *126*, 10370. (g) Schuster, D. I.; Cheng, P.; Jarowski, P. D.; Guldi, D. M.; Luo, C.; Echegoyen, L.; Pyo, S.; Holzwarth, A. R.; Braslavsky, S. E.; Williams, R. M.; Klihm, G. *J. Am. Chem. Soc.* **2004**, *126*, 7257.

(26) Murov, S. I. *Handbook of Photochemistry*; Marcel Dekker: New York, 1985.

(27) Sandanayaka, S. A. D.; Matsukawa, K.; Ishi-i, T.; Mataka, T.; Araki, Y.; Ito, O. *J. Phys. Chem. B* **2004**, *108*, 19995.